DMD Fast Forward. Published on November 18, 2005 as doi:10.1124/dmd.105.005504

DMD #5504

Distribution of ^{14}C-TAS-108 and Its Metabolites after Single Oral Administration to Rats Bearing DMBA-Induced Mammary Tumor

Hidetoshi Yamaya, Mayuko Saeki, Ken-ichiro Yoshida, Jiro Shibata, Shingo Yano, Yoshiaki Sato, Atsushi Takao, Takashi Shindo, Aman U. Buzdar, and Sekio Nagayama

Pharmacokinetics Research Laboratory (H.Y, M.S, K.Y, T.S, N.S), Taiho Pharmaceutical Co., Ltd., Japan; Cancer Research Laboratory (J.S, S.Y), Taiho Pharmaceutical Co., Ltd., Japan; ADME/TOX Research Institute (Y.S, A.T), Daiichi Pure Chemicals Co., Ltd., Japan; The University of Texas M. D. Anderson Cancer Center (A. U. B), Houston, Texas, USA

DMD Fast Forward. Published on November 18, 2005 as DOI: 10.1124/dmd.105.005504
This article has not been copyedited and formatted. The final version may differ from this version.

Running title: Distribution of ^{14}C-TAS-108 in cancerous rats

Corresponding Author:
Hidetoshi Yamaya
Pharmacokinetics Research Laboratory,
Taiho Pharmaceutical Co., Ltd.
224-2 Hiraishi, Ebisuno, Kawauchi-cho
Tokushima 771-0194, Japan
Phone: +(81)-88-665-5337
Fax: +(81)-88-665-6206
Email: hide-yamaya@taiho.co.jp

Pages: 34
Table: 2
Figures: 7
Abstract: 242 words
Introduction: 482 words
Discussion: 947 words

ABBREVIATIONS: ER, estrogen receptor; DMBA, 7,12-dimethylbenz (α)anthracene; SERM, selective estrogen receptor modulator; HPLC, high-performance liquid chromatography; TFA, trifluoroacetic acid; N_2, nitrogen gas; UV, ultra violet; LC/MS/MS, liquid chromatography tandem mass spectrometry; ESI, electrospray ionization; m/z, mass-to-charge ratio; CYP, cytochrome P450; NMR, nuclear magnetic resonance

Abstract

TAS-108 is a novel steroidal anti-estrogen, modulating the differential recruitment of transcriptional co-factors by liganded-ERs, and representing a promising agent for the treatment of breast cancer. To understand better the relationships between the drug exposure and the efficacy or toxicity of TAS-108, we investigated the metabolism and distribution of TAS-108 after oral administration of ^{14}C-TAS-108 to rats bearing a DMBA-induced mammary carcinoma. The metabolites deEt-TAS-108, TAS-108-N-oxide, and TAS-108-COOH were identified as the major metabolites in the plasma; and, additionally, O-Me-deEt-TAS-108 was identified as a novel metabolite in this study. The time-concentration profiles of TAS-108 and its metabolites in the plasma were compared with those in the tumor and uterus of the rats. Radioactivity was found at a high level in various organs including lung, liver, spleen, ovary, and many glands at 12 hr and was relatively higher in tumor tissue than in plasma. On the other hand, the levels of radioactivity in the brain and eyeball were very low or not detectable. TAS-108, deEt-TAS-108, and O-Me-deEt-TAS-108 were extensively distributed in the rat tissues and the tumor, with corresponding tissue/plasma ratios for C_{max} and AUC in the range of 7 to 100.

In contrast, TAS-108-COOH and TAS-108-N-oxide were hardly distributed to the tissues and thus may not contribute to the efficacy or toxicity of TAS-108. Thus, TAS-108, deEt-TAS-108, and OMe-deEt-TAS-108, being distributed highly in tumor tissue, may be more important for the efficacy and toxicity of TAS-108 *in vivo* than TAS-108-COOH and TAS-108-N-oxide.

DMD Fast Forward. Published on November 18, 2005 as DOI: 10.1124/dmd.105.005504
This article has not been copyedited and formatted. The final version may differ from this version.

Introduction

A novel steroidal antiestrogenic compound, TAS-108 (SR16234) has been selected through the biological screening of various newly synthesized steroidal compounds in a collaborative effort between Taiho Pharmaceutical Co., Ltd. and SRI International. TAS-108 has been shown to be a ligand for estrogen receptors (ER) α and β, and its binding affinities are comparable to those of 17β-estradiol (E_2; Yamamoto et al., 2003). The mode of action of TAS-108 on a molecular basis is different from that of E_2; the non-steroidal selective estrogen receptor modulators (SERMs), such as tamoxifen and raloxifene; and the steroidal SERM fulvestrant. The characteristic properties of TAS-108 could present novel biological responses if the concentration of TAS-108 or its metabolites reaches an adequate level in the target tissue. Recently, Ymamoto and coworkers (Yamamoto et al., 2005) reported that TAS-108 at a dosage of 1 to 3 mg/kg/day strongly inhibited tumor growth in rats bearing DMBA-induced mammary carcinoma, the endogenous E_2 model. It is well known that in this model the mammary tumor growth, which depends on endogenous E_2 is suppressed by recently developed anti-estrogenic agents. TAS-108 also strongly inhibited tumor growth in the exogenous E_2 model, in

which tumor growth of MCF-7 xenografts is induced, in mice at a dosage of 1 mg/kg/day without the manifestation of toxicity. On the other hand, in ovariectomized rats administered TAS-108 orally, TAS-108 demonstrated a much weaker estrogenic effect on uterine weight compared with tamoxifen.

The tissue distribution of tamoxifen has been examined in variousanimal studies (Fromson et al., 1973;Major et al., 1976;Ruenitz et al., 1982;Robinson et al., 1991;Toko et al., 1995; Wilking et al., 1982) and clinical studies (Fromson et al., 1973;Lien et al., 1991;Pujol et al., 1995). Although the ratios of tissue versus plasma concentration varied in the reports, the ratios ranged from 8 to 70 for most tissues. As with tamoxifen, non-steroidal SERMs, such as tremifen and TAT-59 (Toko et al., 1995), showed higher concentrations in the tissues than in the plasma or serum. Moreover, tamoxifen is metabolized, and some of the metabolites have been detected in the tumor and tissues. In particular, N-demethyltamoxifen was detected at a higher level in tumor tissue than in plasma in rats and patients (Lien et al., 1989;Lien et al., 1991) and showed a binding affinity similar to that of tamoxifen. The metabolites of tamoxifen have been shown to contribute to the inhibitory effect of the drug.

To understand better the relative contribution of TAS-108 and its metabolites to the efficacy or toxicity of TAS-108, we investigated the metabolism and the distribution of TAS-108 after ^{14}C-TAS-108 had been administered to rats bearing DMBA-induced mammary carcinoma. The time-concentration profile in plasma was compared with that in tumor tissue, which is the target for the activity of TAS-108, and with that in the uterus, the organ that could show adverse side effects. Additionally, we identified several metabolites of TAS-108 and investigated their pharmacokinetic properties in the rats.

Materials and Methods

Materials

TAS-108 (SR16234), which is (7α)-21-[4-[(diethylamino)methyl]-2-methoxyphenoxy]- 7-methyl-19-norpregna-1,3,5(10)-trien-3-ol 2-hydroxy-1,2,3-propanetricarboxylate, and 20,21-$^{13}C_2$- 21,21-D_2-labeled TAS-108 (TAS-108[M+4]) were synthesized at Taiho Pharmaceutical Co., Ltd. (Tokyo, Japan). ^{14}C-labeled TAS-108 (^{14}C-TAS-108), which is (7α)-21-[4-[(diethylamino) methyl]-2-methoxyphenoxy]- 7-methyl-19-norpregna-1, 3,5(10)-trien-3-ol-20-^{14}C 2-hydroxy- 1,2,3-propanetricarboxylate (712 kBq/mg), was synthesized at the ADME/TOX Research Institute, Daiichi Pure Chemicals Co., Ltd. (Ibaraki, Japan). The purity of the labeled and unlabeled compounds was >98.6%. The standard materials (deEt-TAS-108, (7α)-21-[4-[(ethylamino)methyl]-2-methoxyphenoxy]-7-methyl-19-norpregna-1,3,5(10)-trien-3-ol; TAS-108-COOH, 3-methoxy-4-[(7α)-7-methyl-19-norpregna-1,3,5(10)-trien-3-ol-21-yl]oxybenzoic acid; TAS-108-N-oxide, (7α)-21-[4-[(diethylamino)methyl]-2-methoxyphenoxy]-7-methyl-19-norpregna-1, 3,5(10)-trien-3-ol-N-oxide; and O-Me-deEt-TAS-108, (7α)-21-[4-[(ethylamino)methyl]- 2-methoxyphenoxy]-3-methoxy-7-methyl-

19-norpregna-1,3,5(10)-triene), synthesized by Taiho Pharmaceutical Co., Ltd., were used as reference standards for identification of the parent compound and its metabolites. The compound 20,21-$^{13}C_2$- 21,21-D_2-labeled O-Me-deEt-TAS-108 was used as the internal standard for the determination of O-Me-deEt-TAS-108 and was synthesized by Taiho Pharmaceutical Co., Ltd. Carboxymethyl cellulose sodium, disodium hydrogenphosphate, TFA, and S-adenosyl- L-methionine (SAM) were purchased from SIGMA Chemical Co. (Milwaukee, WI). Methanol and acetonitrile were from Kanto Chemical Co. (Tokyo, Japan). Reagents of HPLC grade were used for HPLC.

Animals

Female CD (SD) rats 7 weeks of age were purchased from Charles River Japan Inc. (Hino Farm or Atsugi Farm). For investigating the distribution of TAS-108 in tumorous animals, the rats were treated orally with 7,12-dimethylbenz(α)anthracene (DMBA) at a dose of 20 mg/mL/rat to induce mammary tumors. The length of the major axis of each mammary tumor was measured, and only those animals with a tumor of 17.4–29.0 mm were selected for

this study. The body weights at the dosing of ^{14}C-TAS-108 ranged from 289.0–340.8 g.

Whole-body autoradiography

DMBA-induced mammary tumor-bearing rats were euthanized with an overdose of ether at 2, 6 or 12 hr (n=1) after a single oral administration of ^{14}C-TAS-108 at a dose of 10 mg/kg. The hair was rapidly clipped, and the nasal cavity and anus were filled with 5% carboxymethyl cellulose sodium. The carcass was frozen in a dry ice-acetone mixture. Approximately 35-μm-thick sections were sliced and collected onto adhesive tape and freeze-dried. Each frozen section was covered with a protective membrane and placed in contact with an imaging plate. The imaging plate was then exposed at room temperature for 16 hr in a lead-shielded box. After exposure, the radioactive images on the imaging plate were analyzed by using a bio-image analysis system (BAS2500, Fuji Film Co., Ltd., Tokyo, Japan). The radioactive images were expressed in color grades from 0 to 255 to prepare radioluminograms.

Concentration of radioactivity in plasma, tumor, and uterus

After a single oral administration of ^{14}C-TAS-108 to DMBA-induced mammary tumor-bearing rats at a dose of 10 mg/kg, 3 animals at each time point, 2, 6, 12, 18, 24, 48, and 96 hr, were sacrificed by exsanguination from the abdominal aorta under ether anesthesia. Blood samples were withdrawn into a vacuum tube containing heparin sodium and centrifuged (1800×g, 4°C, 15 min) to separate the plasma. The whole tumors and uterus of each animal were weighed and homogenized with an approximately 4-fold volume of saline. The samples (0.1 mL of plasma, 0.5 mL of tumor homogenate, and 0.5 mL of uterus homogenate) were extracted twice with a 5-fold volume of methanol and centrifuged (1800×g, 4°C, 15 min) to separate the extracted radioactivity from the non-extracted material. Radioactivity in the extraction residue and in the supernatant of the each sample was measured to determine the extraction ratio. The remaining methanol extract was evaporated to dryness with a nitrogen gas stream, and the residue was reconstituted in the solvent containing TAS-108 and the synthetic metabolite standards. The solution was centrifuged (10000×g, 4°C, 15 min), after which the supernatant was subjected to HPLC analysis.

HPLC analysis of TAS-108 and its metabolites

Chromatography was performed on an Inertsil ODS-3 column (5 µm, 4.6 x 250 mm) by using a Shimadzu LC-10A HPLC system. Mobile phases A and B were 20 mmol/L disodium hydrogen phosphate (pH 6.0) and acetonitrile, respectively. The column was run initially at 45% B, and then a linear gradient from 45% B to 60% B was employed between 0 to 30 min, followed by a second linear gradient from 60% B to 90% B applied up to 50 min. Finally an isocratic condition at 90% B was maintained for 10 min. The flow rate was maintained at 1.0 mL/min; and the column temperature, at 40°C. UV detection was performed at 205 nm. Fractions of the HPLC eluate were collected at intervals of 18 sec by using a RETRIEVER IV fraction collector (ISCO, Uppsala, Sweden), and radioactivity in each fraction was determined by liquid scintillation counting after the addition of 4 mL of scintillator Hionic-Fluor^{tm} .

Concentrations of radioactivity in the plasma, tumor, and uterus were expressed as equivalents of TAS-108 (ng eq. /mL or g).

Identification of O-Me-deEt-TAS-108 by LC/MS/MS

We investigated the concentrations of the metabolite *O-Me-deEt-TAS-108* in the liver from 2 normal rats after administration of a mixture of TAS-108 and TAS-108[M+4] (1:1) at the dosage of 30 mg/kg/day for 3 days. The liver was weighed and homogenized in an approximately 4-fold volume of saline. The homogenate was prepared in the same manner as described for the tumor and uterus. Each sample was subjected to preparative HPLC to obtain the fraction containing the target metabolite.

The crude fraction was analyzed by using an LC/MS/MS system comprising a Waters 2690 LC separation module and a Finnigan TSQ7000 tandem mass spectrometer (San Jose, CA) fitted with an ESI interface. The chromatography was performed with methanol containing 15% 10mmol/L ammonium acetate on a CAPCELL PAK C_{18} reversed-phase column (UG-120, 5 μm, 150 × 2.0 mm I.D., Shiseido, Japan). The column was housed in a temperature-regulated compartment maintained at 40°C. The voltage on the ESI interface was maintained at 4.5 kV in the positive-ion mode. For data acquisition, the detector was operated in full-scan mode.

Production of O-Me-deEt-TAS-108 in rat Liver S9 fraction

Twenty-five microliters of rat liver S9 fraction (20 mg protein/mL) was reconstituted in 0.45 mL of 100 mM potassium phosphate buffer (pH 7.4) containing 0.05 mM $MgCl_2$, 0.1 mM EDTA, and various concentrations of deEt-TAS-108 (0.1, 0.3, 1, 3, 10, 30, 50 µg/mL). After 225-µL aliquots of the solutions were taken and the preincubation in a water bath at 37°C for 2 min, reactions were initiated by adding 25 µL of 2000 µM SAM. Blanks contained all the reagents and the substrate except for SAM. Reactions were allowed to proceed for 60 min at 37°C with gentle shaking, and then 150-µL aliquots of the solutions were taken and the reaction terminated by the addition of an equivalent volume of methanol containing the internal standard (10 ng/mL). After the solution had been centrifuged (10000×g, 4°C, 10 min), the supernatant was evaporated to dryness under a stream of a nitrogen gas, and the residue was then reconstituted in the mobile phase of LC/MS/MS. The reconstituted solution was centrifuged (1800×g, 4°C, 5 min), and the resulting supernatant was then analyzed by LC/MS/MS.

Enzyme kinetics parameters were calculated by nonlinear regression analysis to

fit the Michaelis-Menten equation using the enzyme kinetics tool of Sigma plot (version. 7.1, SYSTAT Software Inc., CA, USA).

Pharmacokinetic analysis of TAS-108 and its metabolites

Pharmacokinetic analysis was performed by using WinNonlin (version 3.3, Pharsight Mountain View, CA, USA). The pharmacokinetic parameters observed were the maximum concentration (C_{max}), the time to reach the maximum concentration (t_{max}), the terminal half-life ($t_{1/2}$), and the area under the concentration-time curve (AUC_{0-t}), calculated by using the trapezoidal rule from time 0 to the last time observed.

Results

Whole-body autoradiography

Whole-body autoradiograms were prepared at 2, 6, and 12 hr after a single oral administration of ^{14}C-TAS-108 to DMBA-induced rats at a dose of 10 mg/kg to investigate the tissue distribution of the drug. The overall distribution of radioactivity in the tissues was highest at 6 hr after administration and was comparable at 6 and 12 hr after administration. The levels of radioactivity in the intestinal contents and gastric contents were highest at 12 hr post administration. As shown in the autoradiogram in Fig.1, high levels of radioactivity were seen in the spleen, lung, intestine, mandibular gland, thyroid gland, pancreas, pituitary gland, adrenal gland, liver, ovary, and urinary bladder. The levels of radioactivity in the bone marrow, Harderian gland, stomach, kidney, heart, brown fat, thymus, and tumor were relatively high; whereas those in the uterus and skeletal muscle were low. The skin, blood, fat, and brain showed the lowest radioactivity; and none was detected in the eyeball. The radioactivity in most of the tissues was higher than that in the blood. By investigating the tumor tissue in detail, we found that the radioactivity in the tumor was not in the central necrotic part (Fig. 2), but had

accumulated in the periphery of the tumor at 12 hr.

Determination of O-Me-deEt-TAS-108 as a novel metabolite in tumor and uterus

Showing high tissue distribution, a metabolite of TAS-108 increased in the tumor and uterine tissues with time after administration and was identified from its HPLC retention time as being the same as one of the metabolites found in the plasma. This metabolite was hydrophobic, as judged from a comparison of its HPLC retention time with that of TAS-108; and it was not detected soon after administration, suggesting that this metabolite was formed by further metabolism of deEt-TAS-108, TAS-108-COOH or other metabolites of TAS-108.

The extract of the liver homogenate was analyzed by LC/MS/MS, and its Q1 mass spectrum is shown in Fig. 3. The ion peaks of m/z 492[$M+H^+$] and 496[$M+4+H^+$] were detected at the same signal sensitivity with full-scan monitoring with positive-ionization. To estimate the structure of the metabolite, we examined daughter mass spectra from m/z 492 and 496, which are shown in Fig. 4 (A), (B), respectively; and the characteristics of these fragments are summarized in Table 1. The fragment at m/z 137 was commonly detected with TAS-108 and its metabolites.

The other fragment ion peaks of the remaining steroidal skeleton of the metabolite were +14 shifted. In comparison with the daughter mass spectra of TAS-108 and its metabolites, the liver metabolite was estimated to be O-Me-deEt-TAS-108, which is a methyl conjugate at the phenolic hydroxy group of the steroidal skeleton of deEt-TAS-108. The HPLC retention time of the metabolite was identical with that of synthetic O-Me-deEt-TAS-108 under both analytical HPLC conditions used, i.e., a neutral mobile phase for radioisotope analysis and an acidic mobile phase for LC/MS/MS analysis. Furthermore, the mass spectrum and daughter scan spectrum of synthetic O-Me-deEt-TAS-108 were almost identical with those of the metabolite detected in rat liver.

Metabolism of O-Me-deEt-TAS-108 in rat liver S9 fraction

O-Me-deEt-TAS-108 was formed from deEt-TAS-108 in a rat liver S9 fraction following the addition of SAM. The initial velocity of formation of O-Me-deEt-TAS-108 at each concentration of deEt-TAS-108 is shown in Fig 5. It indicated a typical enzymatic curve of a 1-enzyme reaction according to the Michaelis-Menten model. The Km (Michaelis constant) and Vmax (maximal

DMD Fast Forward. Published on November 18, 2005 as DOI: 10.1124/dmd.105.005504
This article has not been copyedited and formatted. The final version may differ from this version.

velocity) were 8.7 μM (95% confidence interval: 6.0-11.4) and 564.1 fmol/min/mg protein (95% confidence interval: 520.0-608.3), respectively, and the coefficient of determination (R^2) was 0.9829. We concluded that O-Me-deEt-TAS-108 was biotransformed from deEt-TAS-108 enzymatically with a slow rate of biotransformation. Concentrations of O-Me-deEt-TAS-108 were below the quantification limit in control samples lacking SAM, demonstrating that the measured product is not an artifact formed by the extraction vehicle.

Pharmacokinetic profiles of TAS-108 and its identified metabolites in plasma, tumor, and uterus

Recovery of radioactivity from the plasma, tumor, and uterus by the extraction method used (see Materials and Methods) was calculated to be 90.6-98.9%, 97.6-99.5%, and 94.1-97.8%, respectively.

The time-concentration profiles of TAS-108 and its metabolites in plasma, tumor, and uterus are shown graphically in Fig. 6; and those pharmacokinetic parameters are summarized in Table 2. TAS-108-COOH, deEt-TAS-108, and TAS-108-N-oxide were detected as the main metabolites in plasma. The

appearance of O-Me-deEt-TAS-108 lagged behind that of those metabolites, and its low level lasted up to 96 hours. In the tumor, TAS-108-COOH and TAS-108-N-oxide were scarcely detected; and the main metabolites there were OMe-deEt-TAS-108 and deEt-TAS-108. In the uterus, the metabolite profile was similar to that in tumor, but showing slightly lower levels. A few unknown metabolites were detected as minor metabolites.

TAS-108 and deEt-TAS-108 increased to a higher level in the tumor than in the plasma, i.e., 7 and 25 fold, respectively, in terms of Cmax, and 9 and 41 fold, respectively, in terms of AUC. On the other hand, levels of TAS-108-COOH and TAS-108-N-oxide were very low or below the detection level in the tumor tissue. O-Me-deEt-TAS-108 was a main metabolite in the tissues. The tissue/plasma (T/P) ratio for O-Me-deEt-TAS-108 in the tumor tissue was approximately 100-fold higher than the T/P ratio for the parent compound; and this metabolite exhibited a lag in its profile, as found for plasma. Thus, the Tmax was greatly extended, to 48 hours, indicating a slow elimination. These results suggest that a high accumulation of OMe-deEt-TAS-108 would occur with a repeated dose.

Discussion

In the present study, we investigated the distribution of TAS-108 and its metabolites in rats bearing DMBA-induced mammary tumors. TAS-108, a novel antiestrogen agent, is a cationic compound with a steroidal backbone and is synthesized as its citrate salt (Fig. 7). Similar compounds having a highly hydrophobic and cationic side chain, such as a dimethylamino-chain or diethylamino-chain, are well known to achieve a higher concentration in tissue than in plasma (Toko et al., 1995; Dodge et al., 1997). Especially, for compounds that bind ERs, their tissue concentrations are higher in the hormonal organs and are relatively high in estrogen receptor-expressing lung tissue (Kuiper et al., 1997). These properties were confirmed in rats bearing DMBA-induced mammary tumors after administration of TAS-108 at a dose of 10 mg/kg. As was shown in Fig.1, the radioactivity was relatively higher in tumor tissue than in plasma and was found at a high level in lung, liver, ovary, and some glandular tissues at 12 hr after the administration of ^{14}C-TAS-108. In light of the distribution of TAS-108 and its metabolites to the lung and liver, in which metastasized tumor cells are often found, TAS-108 may be expected to inhibit the growth of metastasized cells in breast

cancer patients. On the other hand, the levels of radioactivity in the brain and eyeball were the lowest or not detectable, which would suggest that TAS-108 or its metabolites might not affect the central nervous system or optical system.

In investigating the distribution of radioactivity in the tumor tissue in detail, we found that it was not distributed in the central necrotic part (Fig. 2), but rather had accumulated in the peripheral part of the tumor at 6 and 12 hr. These results suggest that TAS-108 and its metabolites target actively growing cells and thus cause efficient growth inhibition of the tumor (Yamamoto et al., 2005).

We identified TAS-108 and its metabolites in plasma, in the tumor as the target tissue and in the uterus as the organ of the endometrial diseases reported to develop with tamoxifen treatment. TAS-108, deEt-TAS-108, TAS-108-COOH, and TAS-108-N-oxide were identified by HPLC by referring to the standard compounds. In the present study, the main metabolite, O-Me-deEt-TAS-108, in the tissues was identified by LC/MS/MS. By using the stable isotope, we could identify metabolites effectively by using a small volume of a sample. This method may be convenient for identification of some metabolites without the use of radioisotope-labeled compounds. The metabolism of TAS-108 was revealed to involve at least 4

pathways, i.e., N-oxidation, N-deethylation, O-methylation of the phenolic hydroxyl group, and oxidation of N-ethyl- or N-diethyl- group to carboxylic acid. These presumed metabolic pathways are shown in Fig. 7. The metabolic conversion to TAS-108-COOH from TAS-108 or deEt-TAS-108 may occur stepwise via many enzymes including cytochrome P450 (CYP) enzymes. The metabolism to the O-Me-deEt-TAS-108 required SAM as the methyl-supplier in liver S9 fraction, suggesting that O-Me-deEt-TAS-108 was biotransformed by O-methyltransferase.

The metabolites of TAS-108 could be divided into 2 groups based on the characteristics of their distribution: 1) the first group showed a higher distribution in the tumor and uterus than in the plasma. This group has a cationic residue (diethylamino- or ethylamino) in the structure, i.e., deEt-TAS-108, TAS-108, and O-Me-deEt-TAS-108. 2) The second group has anionic residues (N-oxide- or carboxyl-), i.e., TAS-108-N-oxide and TAS-108-COOH, and has a lower distribution in the tissues than in plasma. In the metabolites of the former group, their T/P ratios (ranging from 7 to 48 fold) in terms of C_{max} and AUC were similar to those of tamoxifen (ranging from 10 to 60 fold or over 100 fold) and TAT-59 (range from 19 to 24 fold in AUC; Toko et al., 1995). This property is conducive to inhibition of cell

growth in the target tumor. As deEt-TAS-108 has also been reported to inhibit binding to ER *in vitro* and tumor growth *in vivo* to the same degree as TAS-108 (Shibata et al., 2002), deEt-TAS-108 may contribute to the inhibitory effect on tumor growth following administration of TAS-108.

The T/P ratios of O-Me-deEt-TAS-108 ranged from 48 to 100 in terms of Cmax and AUC, which were considerably higher than those of the other metabolites. Additionally, O-Me-deEt-TAS-108 exhibited a characteristically slow elimination from tissues, suggesting that its accumulation would be high following repeated dosing with TAS-108. . Although the biological activity of O-Me-deEt-TAS-108 was not fully characterized in this present study, from the pharmacokinetic viewpoint, this metabolite may have a great potential to influence the efficacy and safety of TAS-108.

As for TAS-108-COOH and TAS-108-N-oxide of the latter group, because of the poor tissue distribution of these metabolites, their concentrations were apparently higher in plasma due to their small quantity in the whole body, and/or possibly their lower volume of distribution. Although the biological activities of TAS-108-N-oxide and TAS-108-COOH were also not clarified, they may not

contribute to the effect of TAS-108 in rats bearing a DMBA-induced mammary tumor.

In the present study, TAS-108 and deEt-TAS-108, the active metabolite, were extensively distributed in rat tissues and tumor, as indicated by their T/P ratios ranging from 7 to 41. Additionally, O-Me-deEt-TAS-108 also showed extremely high ratios of 48 to 100 in the tissues and tumor. This aspect of TAS-108 and these metabolites is consistent with the high distribution volume of the drug. In contrast, TAS-108-COOH and TAS-108-N-oxide, with their anionic residues, may not contribute to the efficacy or toxicity of TAS-108 because of their low distribution in the tissues. In conclusion, TAS-108 and its hydrophobic metabolites, distributed highly in the tumor tissue, may be more important for the efficacy and toxicity of the drug TAS-108 than those metabolites (TAS-108-COOH, TAS-108-N-oxide) with a lower tissue distribution.

References

Dodge JA, Lugar CW, Cho S, Short LL, Sato M, Yang NN, Spangle LA, Martin MJ, Phillips DL, Glasebrook AL, Osborne JJ, Frolik CA, Bryant HU. (1997) Evaluation of the major metabolites of raloxifene as modulators of tissue selectivity. J Steroid Biochem Mol Biol. 61:97-106

Fromson JM, Pearson S, Bramah S. (1973) The metabolism of tamoxifen (I.C.I. 46,474). I. In laboratory animals. Xenobiotica. 3:693-709.

Fromson JM, Pearson S, Bramah S. (1973) The metabolism of tamoxifen (I.C.I. 46,474). II. In female patients. Xenobiotica. 3:711-714.

Kuiper GG, Carlsson B, Grandien K, Enmark E, Haggblad J, Nilsson S, Gustafsson JA. (1997) Comparison of the ligand binding specificity and transcript tissue distribution of estrogen receptors alpha and beta. Endocrinology. 138:863-70

Lien EA, Solheim E, Lea OA, Lundgren S, Kvinnsland S, and Ueland PM (1989) Distribution of 4-hydroxy-N-desmethyltamoxifen and other tamoxifen metabolites in human biological fluids during tamoxifen treatment. Cancer Res. 49: 2175-2183.

Lien EA, Solheim E, Ueland PM. (1991) Distribution of tamoxifen and its metabolites in rat and human tissues during steady-state treatment. Cancer Res. 51:4837-4844.

Major JS, Green B, Heald PJ. (1976) Interactions of oestradiol-17beta and tamoxifen in the uterus of the pregnant rat. J. Endocrinol. 71:315-24.

Pujol H, Girault J, Rouanet P, Fournier S, Grenier J, Simony J, Fourtillan JB, Pujol JL. (1995) Phase I study of percutaneous 4-hydroxy-tamoxifen with analyses of 4-hydroxy-tamoxifen concentrations in breast cancer and normal breast tissue. Cancer Chemother. Pharmacol. 36:493-498.

Robinson SP, Langan-Fahey SM, Johnson DA, Jordan VC. (1991) Metabolites, pharmacodynamics, and pharmacokinetics of tamoxifen in rats and mice compared to the breast cancer patient. Drug Metab. Dispos. 19:36-43.

Ruenitz PC, Bagley JR. (1985) Comparative fates of clomiphene and tamoxifen in the immature female rat. Drug Metab. Dispos. 13:582-586.

Shibata J., Shindo T., Hashimoto A., Wierzba K., Yamamoto Y., Sakai K., Toko T., Yano S., Matsuo K., Kitazato K. (2002) The anticancer activity of a new antiestrogenic agent, TAS-108 (SR16234), against DMBA-induced

mammary tumors in rats is partly mediated by deEt-TAS-108, its potent metabolite exerting strong antagonistic properties. Eur. J. Cancer, 38, S98.

Toko T, Shibata J, Sugimoto Y, Yamaya H, Yoshida M, Ogawa K, Matsushima E. (1995) Comparative pharmacodynamic analysis of TAT-59 and tamoxifen in rats bearing DMBA-induced mammary carcinoma. Cancer Chemother. Pharmacol. 37:7-13.

Tugnait M, Lenz EM, Phillips P, Hofmann M, Spraul M, Lindon JC, Nicholson JK, Wilson ID. (2002) The metabolism of 4-trifluoromethoxyaniline and [^{13}C]-4-trifluoromethoxyacetanilide in the rat: detection and identification of metabolites excreted in the urine by NMR and HPLC-NMR. J Pharm Biomed Anal. 28:875-885.

Wilking N, Appelgren LE, Carlstrom K, Pousette A, Theve NO. (1982) The distribution and metabolism of ^{14}C-labelled tamoxifen in spayed female mice. Acta Pharmacol. Toxicol. (Copenh). 50:161-168.

Yamamoto Y, Wada O, Takada I, Yogiashi Y, Shibata J, Yanagisawa J, Kitazato K, Kato S (2003) Both N- and C-terminal transactivation functions of

DNA-bound ER are blocked by a novel synthetic estrogen ligand. Biochem. Biophys. Res. Comm. 312:656–662

Yamamoto Y, Shibata J, Yonekura K, Sato K, Hashimoto A, Aoyagi Y, Wierzba K, Yano S, Asao T, Buzdar A U, Terada T (2005) TAS-108, a novel oral steroidal antiestrogenic agent, is a pure antagonist on estrogen receptor α and a partial agonist on estrogen receptor β with low uterotrophic effect. Clin. Cancer Res. 11:315-322

Figure Legends

Fig. 1 Autoluminograph of DMBA-induced mammary tumor bearing rat at 12 hr after oral administration at a dose of 10 mg/kg. 1. Adrenal gland, 2. Blood, 3. Bone marrow, 4. Brain, 5. Brown fat, 6. Eyeball, 7. Fat, 8. Gastric contents, 9. Harderian gland, 10. Heart, 11. Intestinal contents, 12. Intestine, 13. Kidney, 14. Liver, 15. Lung, 16. Mandibular gland, 17. Ovary, 18. Pancreas, 19. Pituitary gland, 20. Skeletal muscle, 21. Skin, 22. Spleen, 23. Stomach, 24. Thymus, 25. Thyroid gland, 26. Tumor, 27. Urinary bladder, 28. Uterus. The color bar shows the radioactive intensity according to the luminogram indicator.

Fig. 2 Typical radioluminograms of a tumor at each time point after single oral administration of ^{14}C-TAS-108 (dose: 10 mg/kg)

Fig. 3 Mass chromatograms and mass spectrum of methanol extract

Crude fraction of a methanol extract was prepared from rat liver after the

administration of TAS-108 and TAS-108[M+4].

Fig. 4 Daughter mass spectra from m/z 492 (A) and m/z 496 (B) in the positive-ion scan mode. The insert diagrams show the position of ion fragmentation and a mass-to-charge ratio of each fragment.

Fig. 5 The initial velocity of biotransforming O-Me-deEt-TAS-108 at each concentration of deEt-TAS-108 in the rat liver S9 fraction. This enzyme kinetic parameter was calculated by using duplicate data.

Fig. 6 Time-dependent concentration profiles of TAS-108 and its metabolites in plasma (A), tumor (B), and uterus (C) after the oral administration to DMBA-induced mammary tumor-bearing rats. The symbols indicate TAS-108 (closed circle), deEt-TAS-108 (closed triangle), TAS-108-N-oxide (open triangle), TAS-108-COOH (open circle), O-Me-deEt-TAS-108 (closed diamond), unknown 1 (closed square), and unknown 2 (open square). The animals were given TAS-108 at a dose of 10 mg/kg. All concentrations are presented as the mean values of 3 animals, and

were calculated as the equivalents of TAS-108.

Fig. 7 Presumed metabolic pathways in rats bearing DMBA-induced mammary tumor. The broken arrow indicates that the metabolic pathway is estimated to be caused by stepwise metabolism.

Tables

Table 1. Comparison of the fragments in the daughter mass spectrum between the subject metabolite and TAS-108 and its known metabolites.

	The subjective metabolite	The subjective metabolite [M+4]	TAS-108	deEt-TAS108	TAS-108-N-oxide
Q1	491(477+14)	495(491+4)	509	477	528
F1	137	137	137	137	137
F2	161(147+14)	161	147	147	147
F3	187 (173+14)	187	173	173	173
F4	311 (277+14)	315(311+4)	277	277	277
F5	447 (433+14)	451(447+4)	433	433	433

The daughter mass spectra of TAS-108 and its known metabolites were obtained with a Finnigan TSQ 7000 detector according to the description in the Methods section.

Table 2. Summary of pharmacokinetic parameters of TAS-108 and its known metabolites in plasma, tumor, and uterus.

	Tmax	Cmax	AUC0-t	Apparent t1/2
	(hr)	(ng eq./mL or ng eq./g)	(ng eq.·hr/mL or ng eq.·hr/g)	(hr)
Plasma				
TAS-108	2	56	554(0-24)	4.1(12-24)
deEt-TAS-108	6	32	442(0-24)	4.7(12-24)
TAS-108-COOH	6	65	1230(0-96)	20(24-96)
TAS-108-N-oxide	6	40	317(0-12)	-
O-Me-deEt-TAS-108	18	16	877(0-96)	-
Tumor				
TAS-108	6	400	5200(0-24)	5.8(12-24)
deEt-TAS-108	12	811	18100(0-48)	13(18-48)
TAS-108-COOH	12	24	306(0-24)	12(12-24)
TAS-108-N-oxide	-	-	-	-
O-Me-deEt-TAS-108	48	1401	87686(0-96)	-
Uterus				
TAS-108	6	245	2810(0-24)	-
deEt-TAS-108	12	530	7290(0-24)	7.7(12-24)
TAS-108-COOH	12	41*	-	-
TAS-108-N-oxide	-	-	-	-
O-Me-deEt-TAS-108	48	761	55274(0-96)	-

*The value shown is the mean of 2 animals detected only at 12 hr, -: not calculated
The values in parentheses represent the ranges of time points used for calculation.

DMD Fast Forward. Published on November 18, 2005 as DOI: 10.1124/dmd.105.005504
This article has not been copyedited and formatted. The final version may differ from this version.

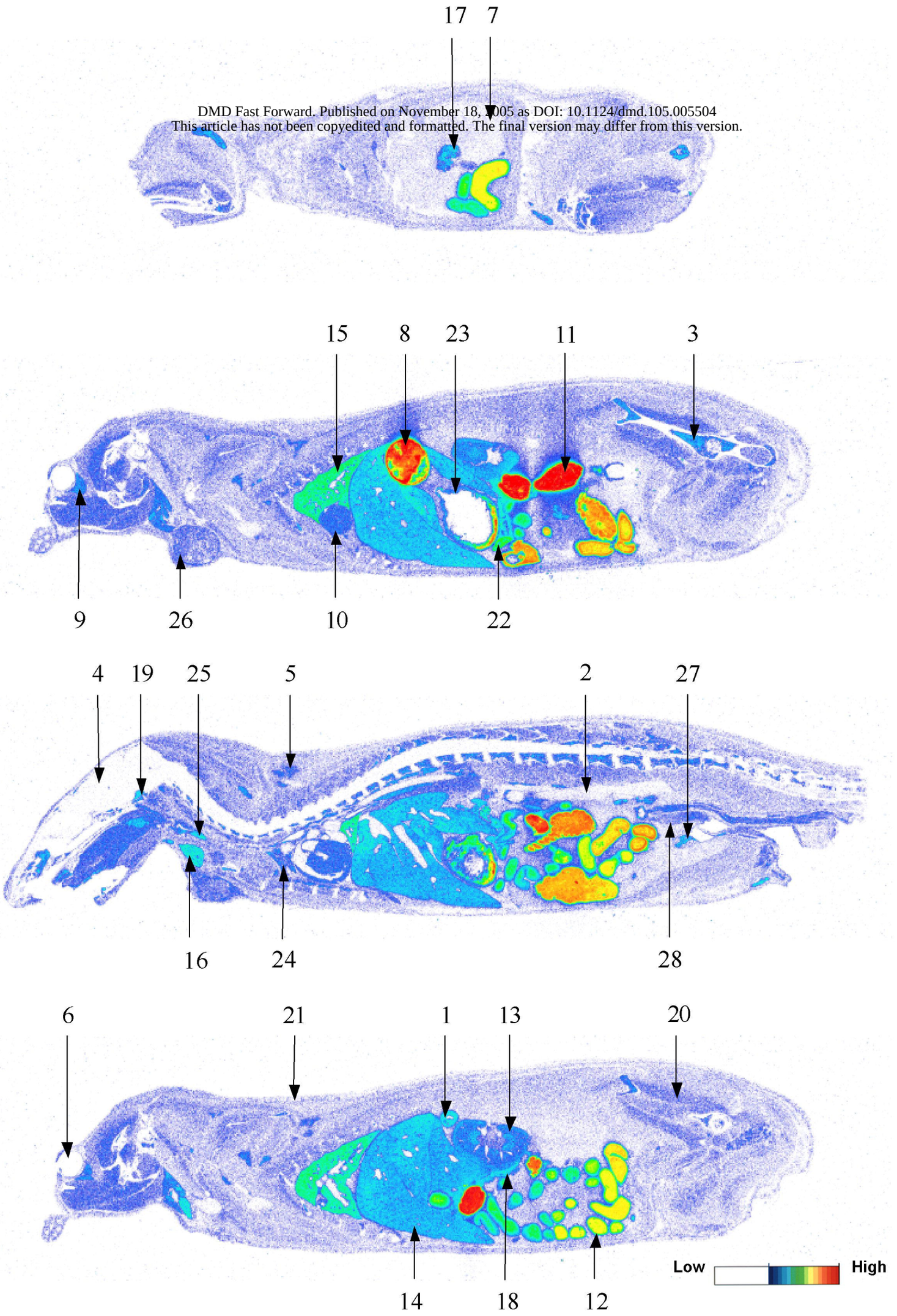

Fig. 1

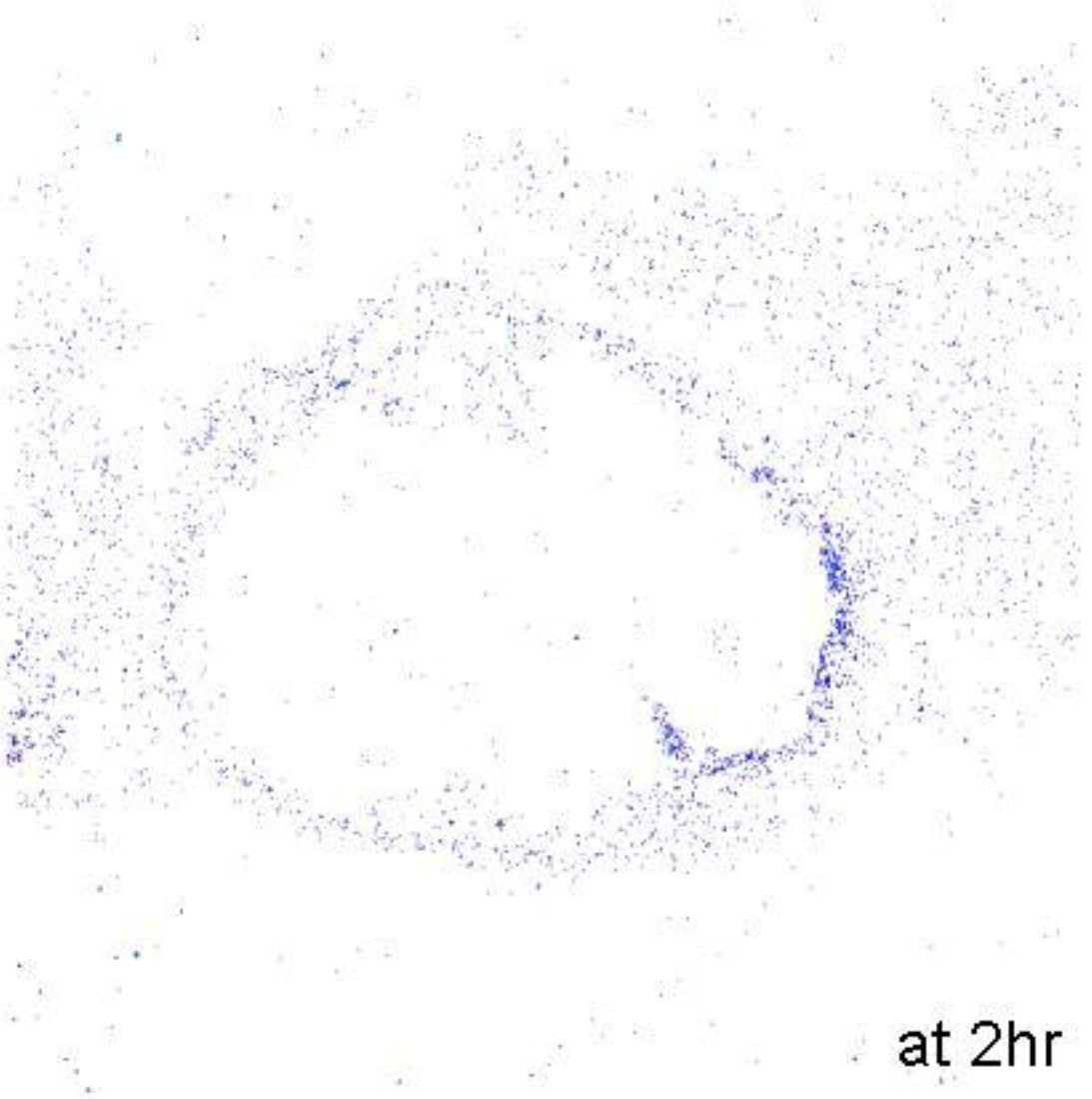

Fig. 2(A)

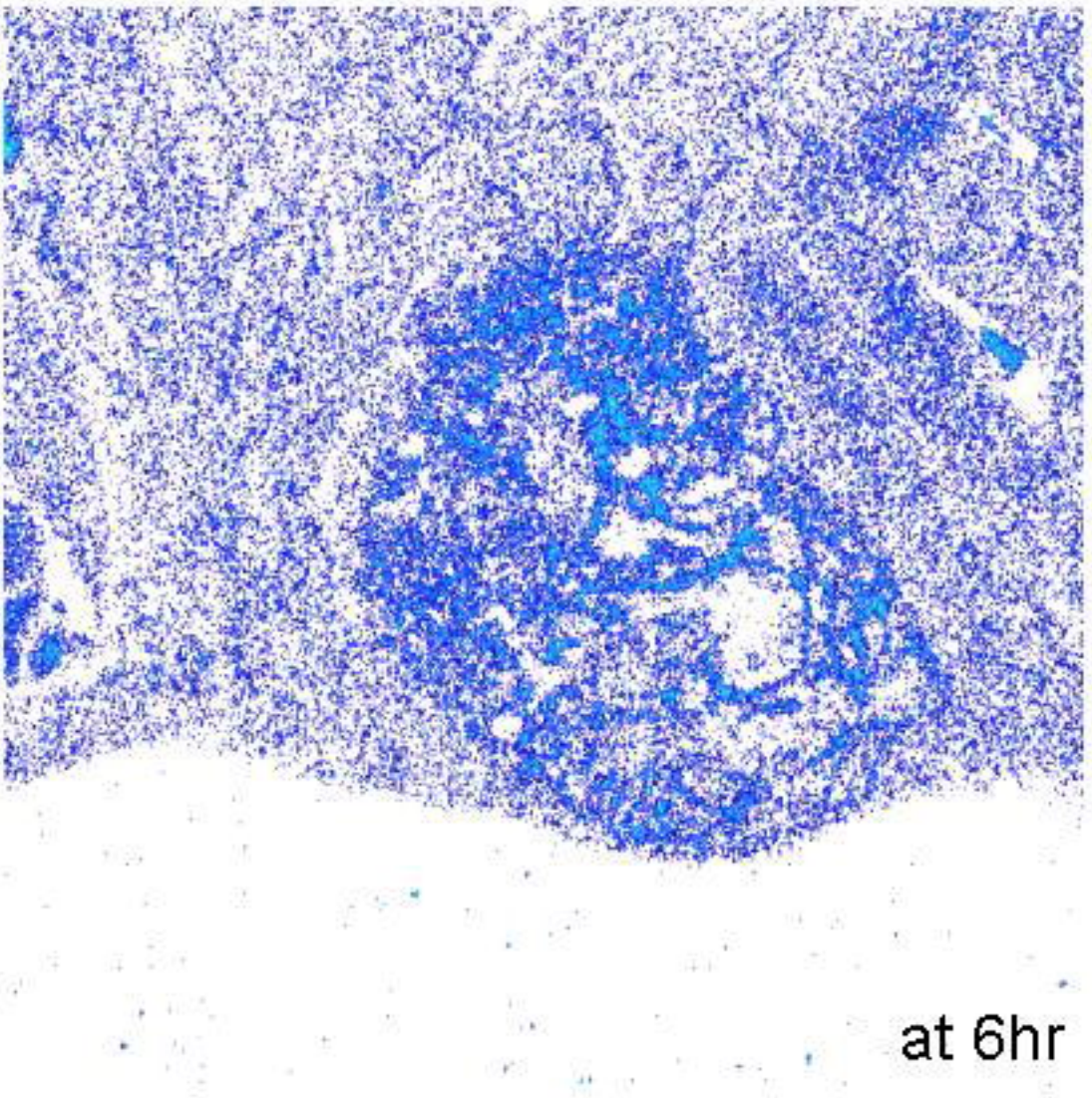

Fig. 2(B)

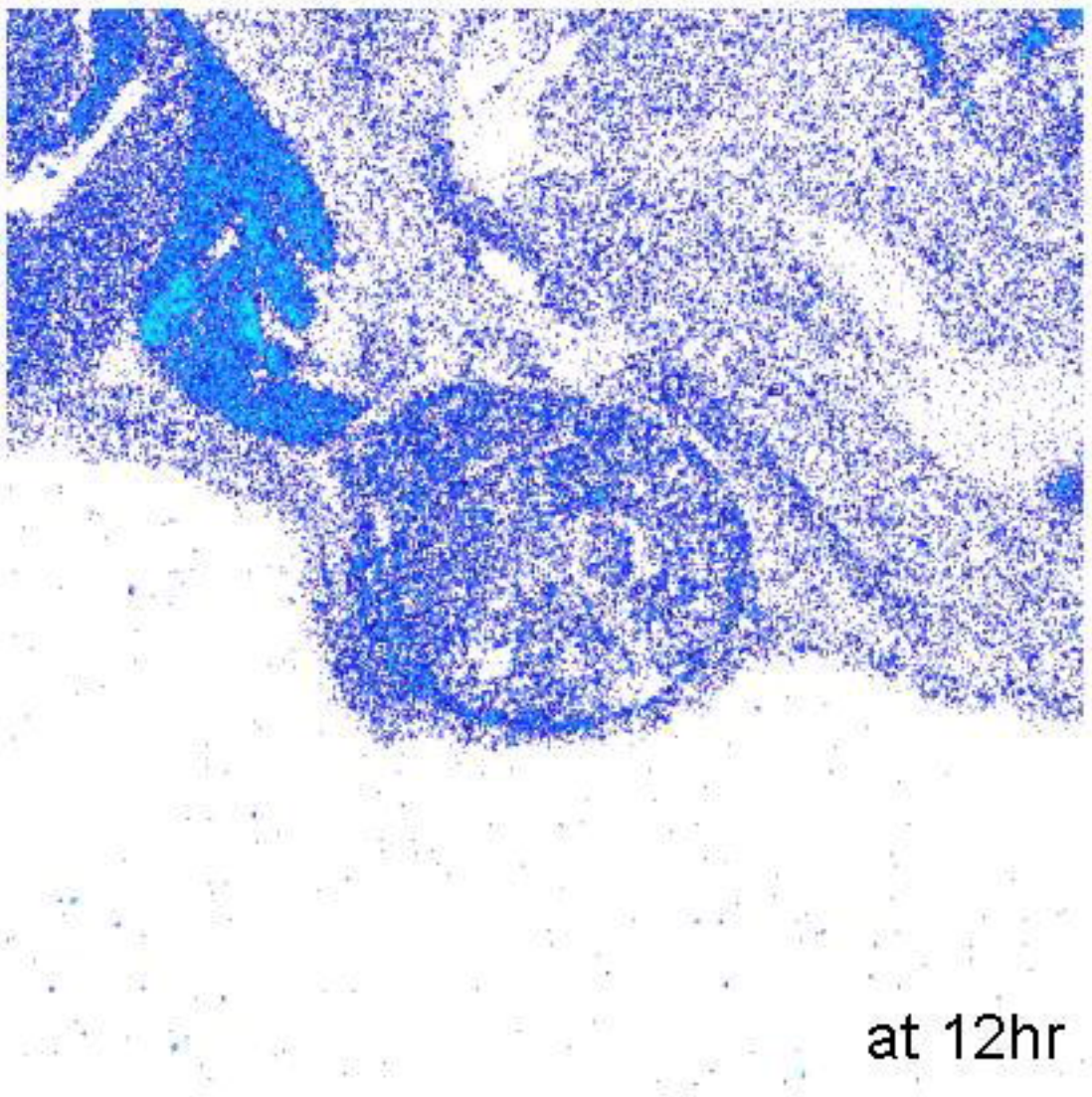

Fig. 2(C)

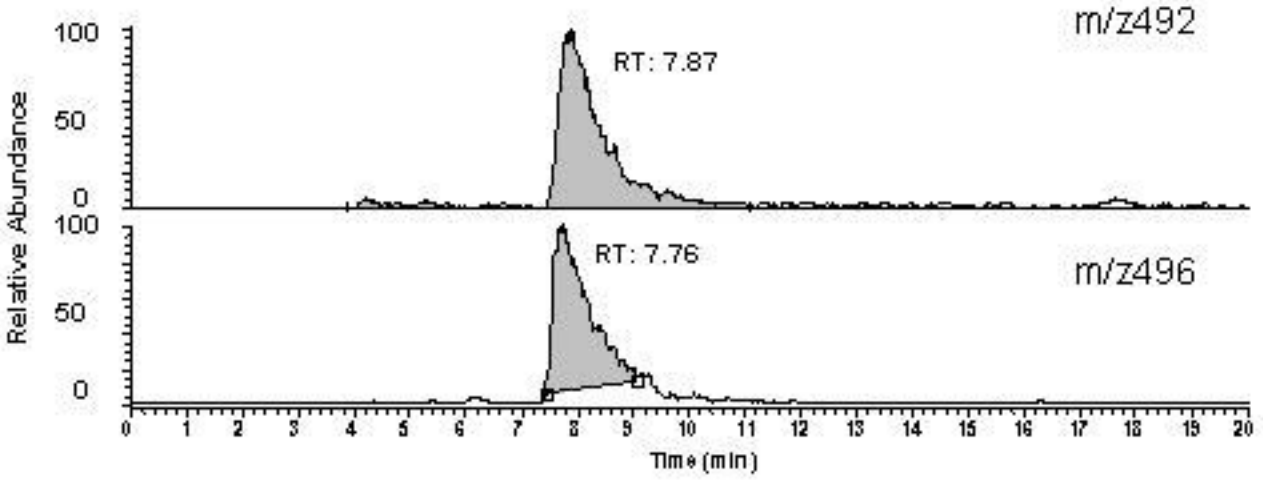
m/z492
RT: 7.87
RT: 7.76
m/z496
Relative Abundance
Time (min)

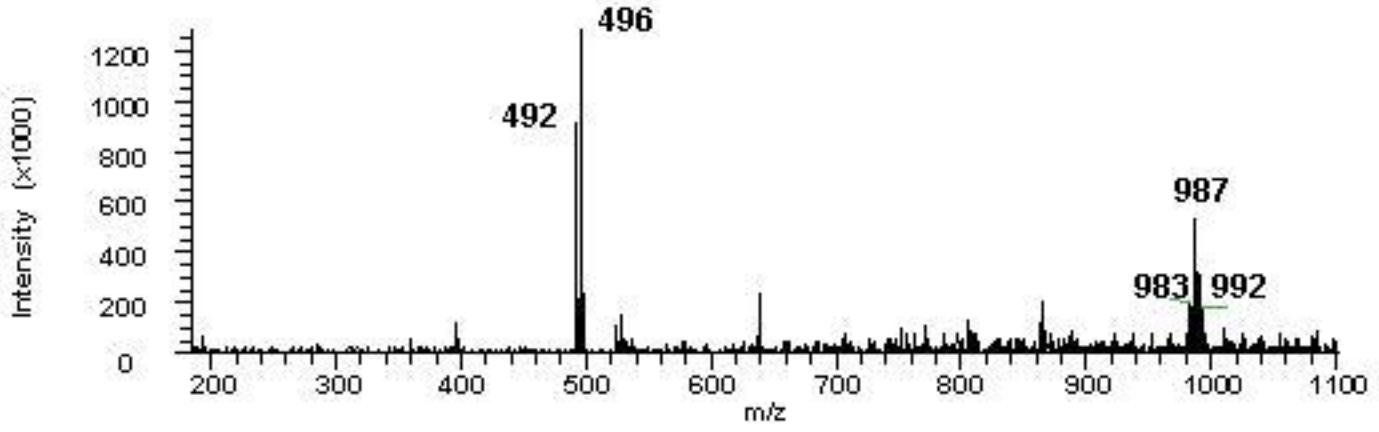
496
492
987
983
992
Intensity (x1000)
m/z

Fig. 3

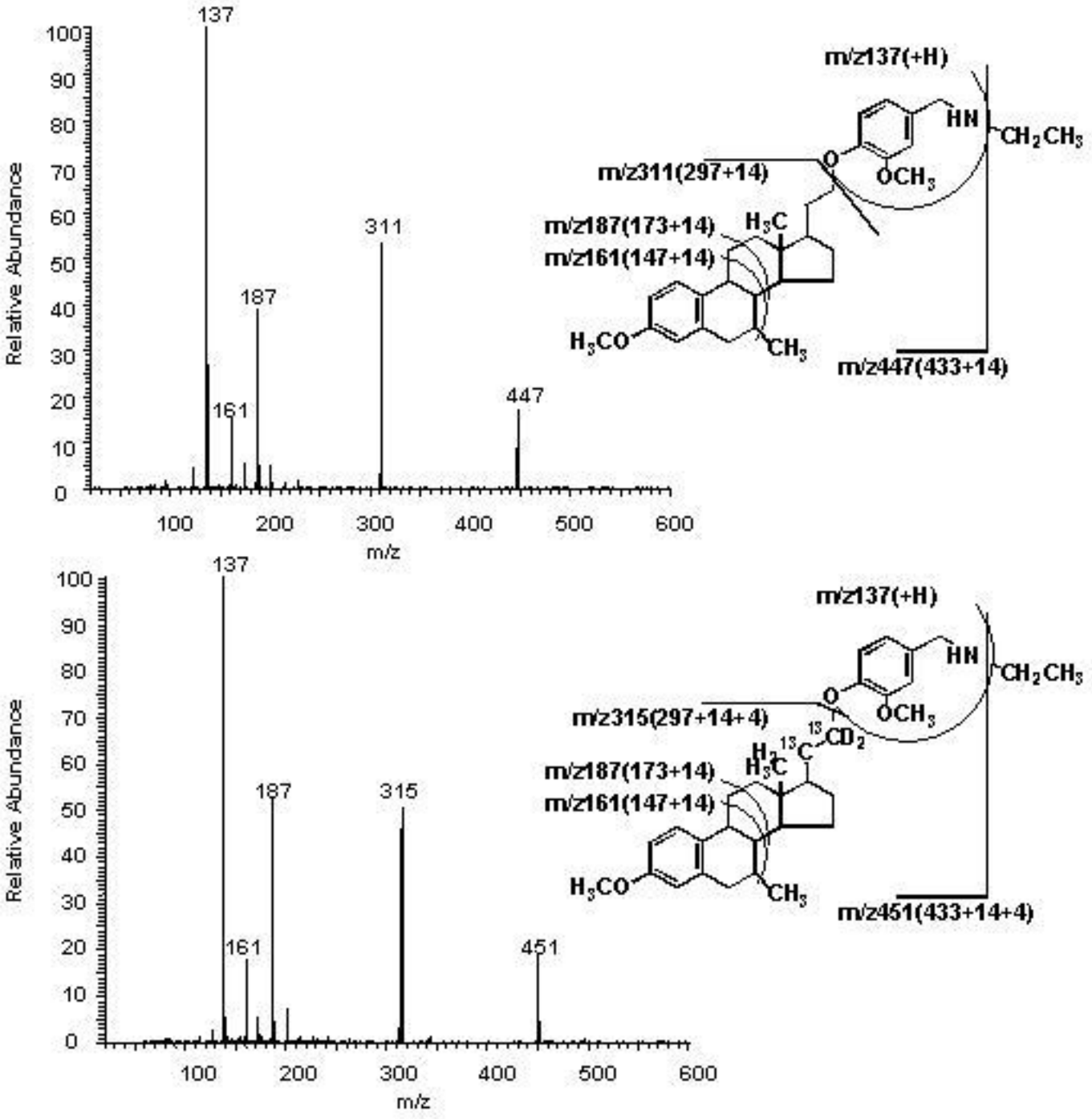
137
311
187
161
447
Relative Abundance
m/z
m/z137(+H)
m/z311(297+14)
m/z187(173+14)
m/z161(147+14)
m/z447(433+14)
HN
CH2CH3
OCH3
H3C
H3CO
CH3
315
451
m/z315(297+14+4)
m/z451(433+14+4)
13CD2
13C

Fig. 4

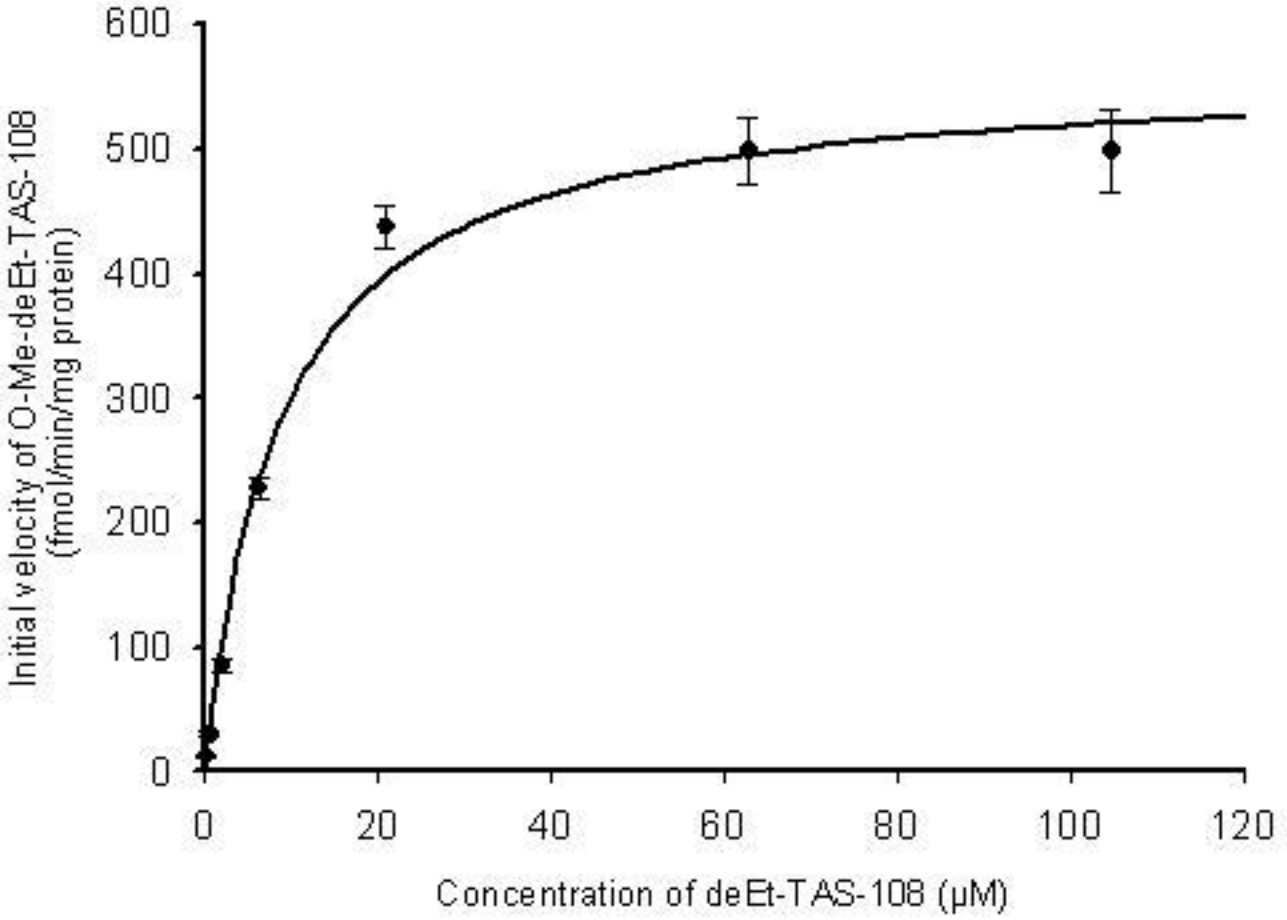
600
500
400
300
200
100
0
Initial velocity of O-Me-deEt-TAS-108 (fmol/min/mg protein)
0
20
40
60
80
100
120
Concentration of deEt-TAS-108 (μM)

Fig. 5

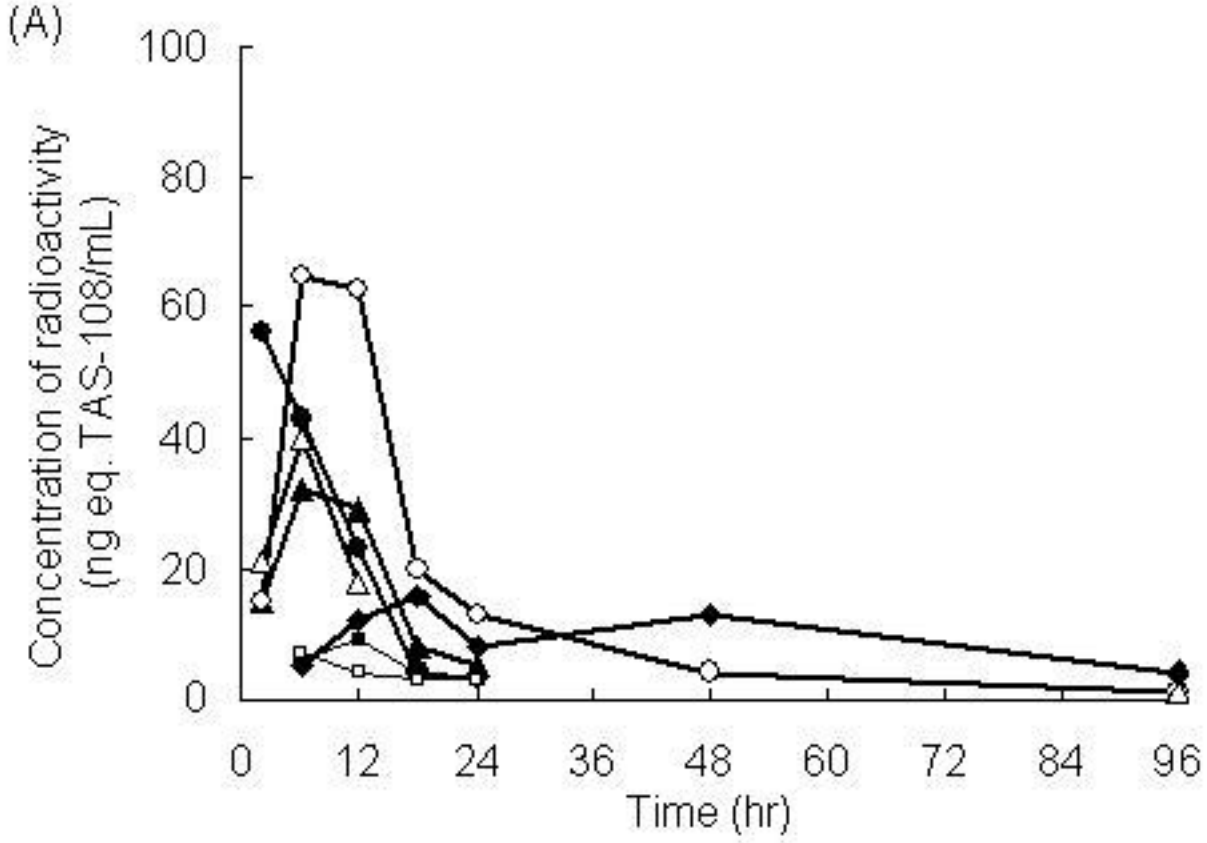
(A)
Concentration of radioactivity (ng eq. TAS-108/mL)
100
80
60
40
20
0
0
12
24
36
48
60
72
84
96
Time (hr)

Fig. 6

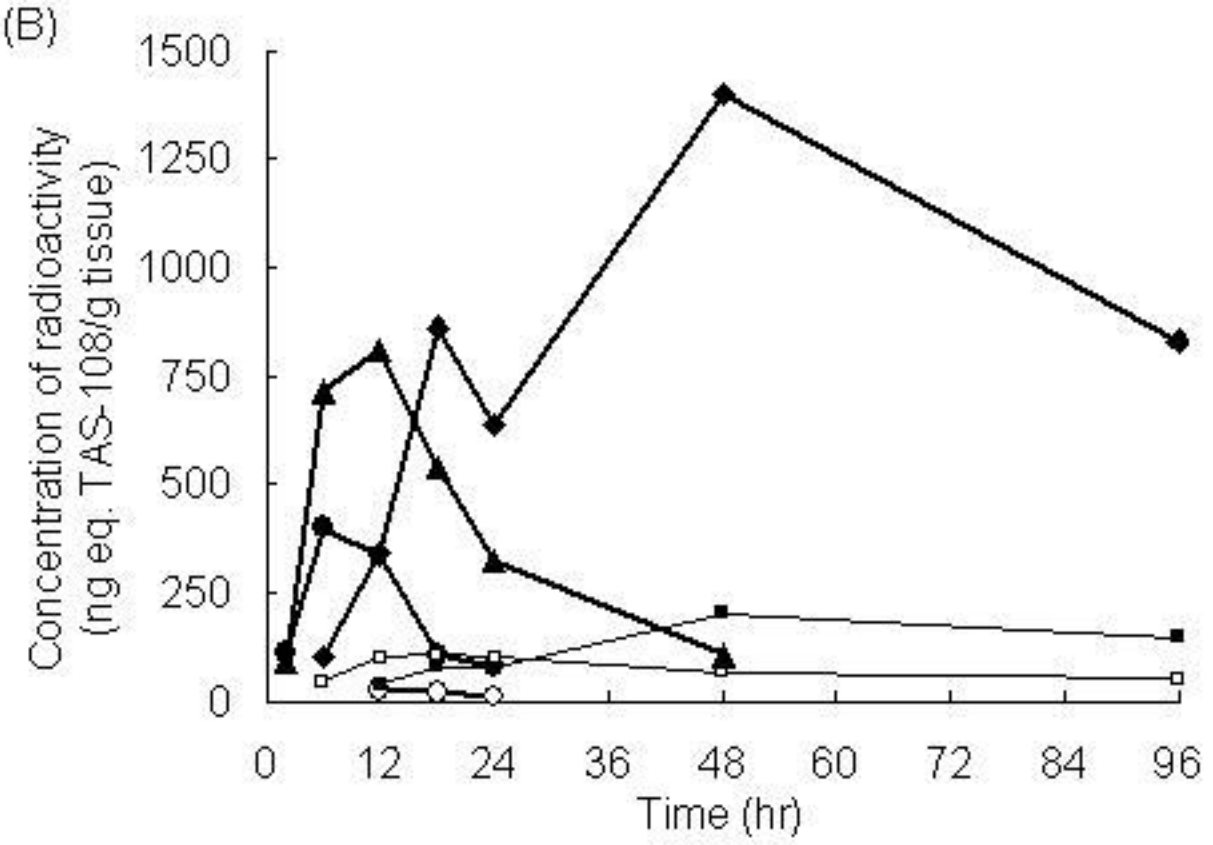
(B)
Concentration of radioactivity (ng eq. TAS-108/g tissue)
1500
1250
1000
750
500
250
0
0
12
24
36
48
60
72
84
96
Time (hr)

Fig. 6

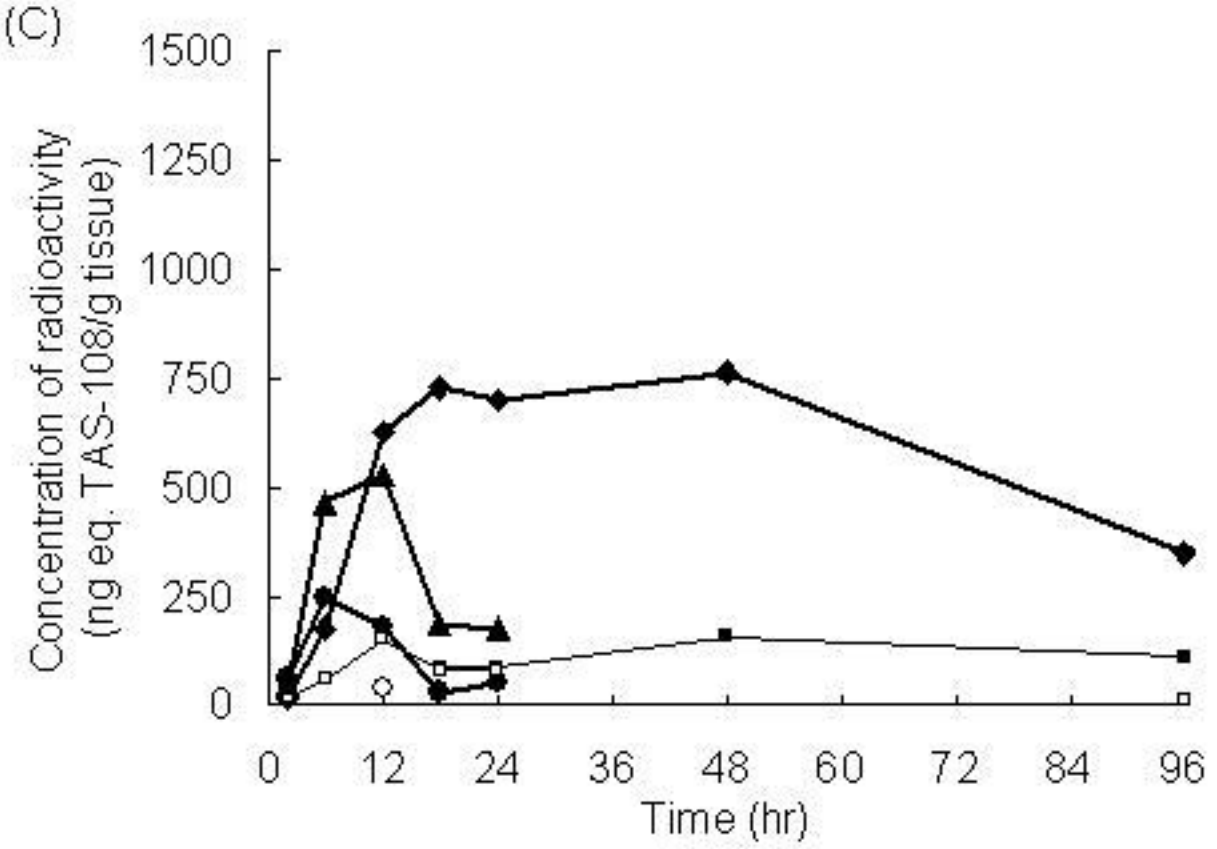
(C)
Concentration of radioactivity (ng eq. TAS-108/g tissue)
1500
1250
1000
750
500
250
0
0
12
24
36
48
60
72
84
96
Time (hr)

Fig. 6

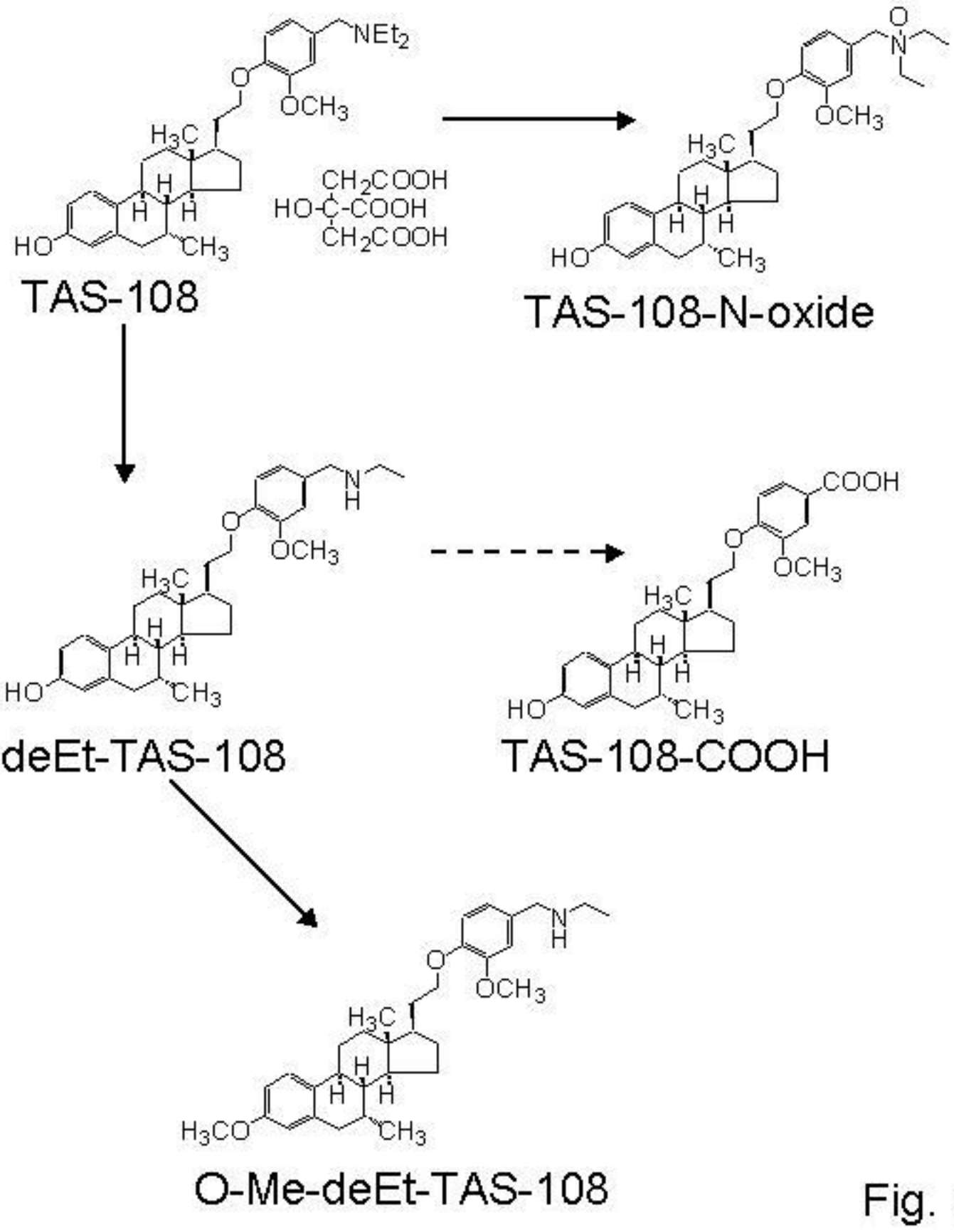
NEt2
OCH3
H3C
H
HO
CH3
CH2COOH
HO-C-COOH
CH2COOH
TAS-108
O
N
TAS-108-N-oxide
deEt-TAS-108
COOH
TAS-108-COOH
H3CO
O-Me-deEt-TAS-108

Fig. 7